

## Research Paper

## Flow and heat transfer model for turbulent-laminar/turbulent gas-liquid annular flows

Shaotong Jia<sup>b</sup>, Chuanshuai Dong<sup>a,\*</sup><sup>a</sup> Key Laboratory of Enhanced Heat Transfer and Energy Conservation of Education Ministry, School of Chemistry and Chemical Engineering, South China University of Technology, Guangzhou 510640, China<sup>b</sup> China Oil and Gas Pipeline Network Corporation, Guangzhou 510620, China

## ARTICLE INFO

## ABSTRACT

## Keywords:

Gas-liquid two-phase flow  
Heat transfer coefficient  
Annular flow  
Void fraction

Two-phase gas-liquid annular flows are characterized by the liquid flowing in the annular-shaped channels as liquid film and gas flowing in the center as gas core. Adequate understanding of the flow and heat transfer mechanism is important. This paper aims at developing a model for flow and heat transfer in two-phase annular flows. First, the physical process of flow and heat transfer for two-phase annular flow is mathematically formulated and a new heat transfer model is developed based on two-fluid concept. Then, the new model is well validated using the experimental void fraction, liquid film thickness, and heat transfer coefficient collected from various sources. Third, the effect of the orientations and flow parameters on the heat transfer of two-phase annular flows are comprehensively investigated. Finally, the dependence of the two-phase heat transfer multipliers on the void fractions and pressure multipliers is identified quantitatively and a simple heat transfer correlation is developed based on Chilton & Colburn analogy.

## 1. Introduction

Two-phase gas liquid flows are widely found in many natural and engineering fields, such as chemical columns and petroleum pipelines. Due to the deformable interface between liquid and gas phases, depending on physical properties, gravity, flow velocities, and orientations of the flow channel, etc., two-phase flow is very complicated [51,55,9]. The phenomenon occurring in two-phase flows are too complex to be amenable to a rigorous mathematical solution [44,23,33]. Amongst the main flow regimes, two-phase annular flows are widely encountered in many fields, such as evaporators, condensers, and boiling-water reactors [38]. Two-phase annular flows are characterized by the continuous annular liquid film flowing on the channel wall and gas travelling through in the gas core. The annular liquid film could be entrained into the gas core and disintegrated into small liquid droplets at high gas velocities [54]. Meanwhile, the liquid droplet in the gas core might deposit on the liquid film [28].

Considering the importance of two-phase flow, tremendous efforts are made in understanding its flow mechanism [7,1,27,22,21]. Several models of two-phase flow are proposed. Homogeneous flow models, drift-flux models, two-fluid models, and flow regime-based models are often used in two-phase flow simulation. The central assumption in

homogenous flow model is that gas and liquid are considered as homogenous single pseudo-fluids [6,35]. Thus, the homogenous flow is not suitable in two-phase annular flows because of its distinct interface and huge difference of velocities between liquid and gas phases. The drift-flux model is characterized by the consideration of relative movement between gas and liquid using a constitutive relation [15]. In two-fluid model, gas and liquid are considered as continuous fully-separated flows [46,8]. To consider the deformable interface and complicated interaction between gas and liquid, a flow regime-based model is proposed for the specific flow regime.

The flow behavior of annular liquid film is of key importance in two-phase annular flows [31,24]. He et al. [22,21] investigated the local liquid film behavior of annular flows on rod-bundle orientations and proposed a mechanistic model for calculating the local film thickness and spatial distribution of gas flow. Fan et al. [16] performed both experimental and numerical investigation on the formation and development of disturbance waves in annular flows. Ju et al. [25] and Wang et al. [48] investigated the wave characteristics of vertical annular flows and developed models for calculating the wave velocity, and wave height.

Owing to the flow complexity of annular flows, the heat transfer process is much more complicated. Keniar and Gerimella (2021) proposed a mechanistic model for calculating the condensation heat

\* Corresponding author.

E-mail address: [dongcs@scut.edu.cn](mailto:dongcs@scut.edu.cn) (C. Dong).

Nomenclature		
$A$	Area [ $\text{m}^2$ ]	$\theta$ Inclination angle [ $^\circ$ ]
$C_p$	Specific heat capacity [ $\text{kJ}/(\text{kg}\cdot\text{K})$ ]	$\mu$ Dynamic viscosity [ $\text{Pa}\cdot\text{s}$ ]
$d$	Diameter [m]	$\rho$ Density [ $\text{kg}/\text{m}^3$ ]
$D$	Hydraulic diameter [m]	$\tau$ Shear stress [N/m]
$f$	Friction factor [-]	$\Phi_f^2$ Two-phase pressure drop multiplier [-]
$g$	Gravitational acceleration [ $\text{m}/\text{s}^2$ ]	$\Phi_h^2$ Two-phase heat transfer multiplier [-]
$h$	Heat transfer coefficient [ $\text{W}/(\text{m}^2\cdot\text{K})$ ]	
$k_s$	Surface roughness [m]	
$L$	Length [m]	
$L_t$	Thermal entrance length [m]	
$m$	Mass flow rate [ $\text{kg}/\text{s}$ ]	
$Nu$	Nusselt number [-]	
$P$	Pressure [Pa]	
$Pr$	Prandtl number [-]	
$q$	Heat flux [ $\text{W}/\text{m}^2$ ]	
$Re$	Reynolds number [-]	
$S$	Perimeter [m]	
$T$	Temperature [ $^\circ\text{C}$ ]	
$V$	Velocity [m/s]	
<i>Greek Symbols</i>		
$\alpha$	Void fraction [-]	
$\delta$	Liquid film thickness [m]	
$\varepsilon$	Entrainment rate [-]	
<i>Subscripts</i>		
$C$	Gas core [-]	
$D$	Liquid droplet [-]	
$F$	Liquid film [-]	
$G$	Gas [-]	
$i$	Inner [-]	
$I$	Interface [-]	
$L$	Liquid [-]	
$m$	Gas-liquid mixture [-]	
$MCD$	Mixed convection [-]	
$o$	Outer [-]	
$s$	Surrounding [-]	
$sim$	Simulated [-]	
$SL$	Superficial liquid [-]	
$SG$	Superficial gas [-]	
$W$	Wall [-]	
$1\phi$	Single phase [-]	
$2\phi$	Two phase [-]	

transfer coefficients of intermittent and annular flow regimes. The model was developed using the laminar assumption and applicable to arbitrarily shaped micro- or mini-channels. Thome et al. [26,43] developed a flow-regime based models for two-phase flows. Zhang et al. [52] proposed a unified heat transfer model for various flow regimes but did not investigated the influence of flow parameters and orientations on the heat transfer process.

Recently, we have developed a series of mechanistic models of flow and heat transfer for gas-liquid two-phase slug flow and stratified flow [12,13,14]. Considering the periodic flow behaviors of two-phase slug flows in horizontal and vertical pipes, its mechanistic models were developed based on the slug unit cell concept. For two-phase stratified flows, the mechanistic model was developed based on the two-fluid model because of the distinct interface between gas and liquid. Both the gas and liquid contacts with the pipe wall in two-phase stratified flow. However, as the velocity of the gas increases, the liquid is blown by the gas and finally forms a continuous annular film on the pipe wall. Thus, there exists huge difference in the flow and heat transfer between two-phase annular flow and stratified flow.

Considering the importance of two-phase annular flow and its

unclear mechanism of heat transfer enhancement by the injection of gas into liquid, this study aims at developing a model of flow and heat transfer for two-phase annular flows to investigate the mechanism of the heat transfer enhancement comprehensively. The physical process of flow and heat transfer is formulated mathematically.

## 2. Hydrodynamic model

As shown in Fig. 1, the annular liquid film flows continuously on the annulus-shaped channel wall, while the gas flows in the gas core, carrying varying amounts of liquid droplets. The two regions are separated by a distinct interface. The annular liquid film becomes wavy and part of the liquid might be entrained in the gas core at high gas velocity. Because of the gravity effect, the annular liquid film in the top is usually thinner than that in the bottom in horizontal and inclined pipes. Such difference becomes small and thus uniform film thickness around the pipe periphery is adopted in this model [44]. The formulation of the hydrodynamic model is developed based on continuity and momentum equations of both liquid and gas.

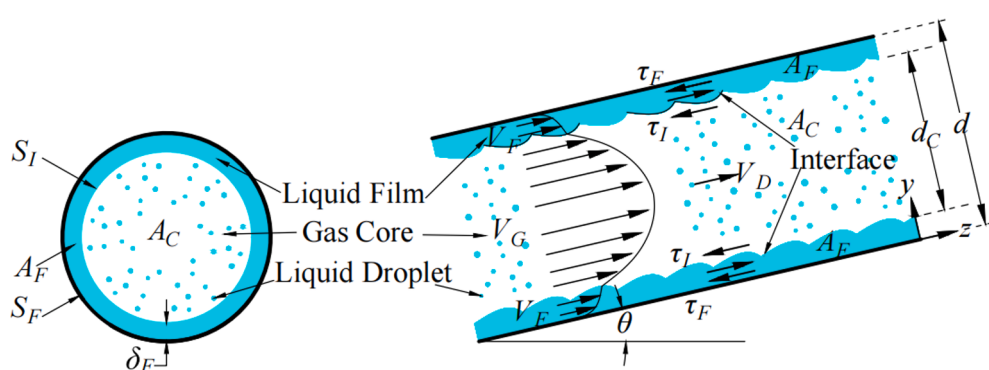


Fig. 1. Schematic of the two-phase annular flows.

## 2.1. Continuity equations

The liquid phase flows in the annular liquid film region as continuous liquid film and in the gas core region as entrained liquid droplet. Thus, the continuity equation of the liquid phase is given by:

$$m = \rho_L V_{SL} A = m_F + m_D = \rho_L V_F A_F + \rho_L V_D A_D \quad (1)$$

where  $m$ ,  $m_F$ , and  $m_D$  are the mass flow rates of the liquid in the whole flow channel, annular liquid film region, and gas core, respectively.  $\rho_L$  is the density of the liquid.  $V_{SL}$  is the superficial liquid velocity.  $A$ ,  $A_F$ , and  $A_D$  are the cross-sectional areas of the whole channel, the annular liquid film region, and the entrained liquid droplet, respectively.  $V_F$  and  $V_D$  are the flow velocities of the annular liquid film and liquid droplet.

$A_F$  is given by:

$$A_F = \frac{\pi}{4} [d^2 - (d - 2\delta)^2] \quad (2)$$

where  $\delta$  is the liquid film thickness. Due to the rather small thickness of the liquid film,  $A_F$  can also be approximately estimated by:

$$A_F = \pi d \delta \quad (3)$$

$A_D$  is given by:

$$A_D = A_C (1 - \alpha_C) \quad (4)$$

where  $\alpha_C$  refers to the void fraction of the gas core and  $A_C$  refers to the cross-sectional area.

$$A_C = \frac{1}{4} \pi (d - 2\delta)^2 \quad (5)$$

The void fraction in the gas core,  $\alpha_C$ , is defined by:

$$\alpha_C = 1 - \frac{A_D}{A_C} = 1 - \frac{\varepsilon m_L / \rho_L / V_D}{A - \pi d \delta} = 1 - \frac{\varepsilon V_{SL} / V_D}{1 - \frac{4}{d} \delta} \quad (6)$$

where  $V_D$  is the velocity of the liquid droplet. Due to the much smaller size of the liquid droplet, the velocity of the liquid droplet is assumed to be equal to the actual gas velocity.  $\varepsilon$  is a measure of the fraction of liquid that flows in the gas core, calculated by Wallis correlation [47].

$$\varepsilon = 1 - e^{-0.125(\phi-1.5)} \quad (7)$$

where  $\phi$  is defined as:

$$\phi = 10^4 \frac{V_{SG} \mu_G}{\sigma} \left( \frac{\rho_G}{\rho_L} \right)^{0.5} \quad (8)$$

Due to the small film thickness and quite low flow velocity, little gas bubbles are contained in the annular liquid film and therefore the gas phase only flows at the gas core region. Thus, the continuity equation of the gas phase is given by:

$$\rho_G V_{SG} A = \rho_G V_G A_C \alpha_C \quad (9)$$

Or

$$V_{SG} A = V_G A_C \alpha_C \quad (10)$$

where  $V_{SG}$  is the superficial velocity of gas and  $V_G$  is the actual gas velocity in the gas core.

## 2.2. Momentum equations

The momentum equation of the annular liquid film is formulated by:

$$-A_F \frac{dP}{dz} - \tau_F S_F + \tau_I S_I - \rho_F A_F g \sin \theta = 0 \quad (11)$$

where  $A_F$  is the cross-sectional area of the annular liquid film region.  $\frac{dP}{dz}$  is

the pressure drop.  $S_F$  and  $S_I$  are the wet perimeters.  $\tau_F$  and  $\tau_I$  are the shear stresses.  $\theta$  is the inclination angle from the horizontal orientations, where  $\theta = 0^\circ$  is assumed for flow in horizontal pipes,  $\theta > 0^\circ$  is assumed for flow in upward inclined pipes, and  $\theta < 0^\circ$  is assumed for flow in downward inclined pipes.

Varying amount of liquid droplets are entrained in the gas core. To simply the model, the gas core is assumed as a homogeneous single pseudo-fluid. Therefore, the momentum equation of the gas core is given by:

$$-A_C \frac{dP}{dz} - \tau_I S_I - \rho_C A_C g \sin \theta = 0 \quad (12)$$

where  $\rho_C$  is the mixture density, estimated by:

$$\rho_C = \alpha_C \rho_G + (1 - \alpha_C) \rho_L \quad (13)$$

where  $\alpha_C$  is the void fraction of the gas core.  $\alpha_C = 1$  means that no liquid droplets are contained in the gas core. Owing to the equal pressure drops in the gas core and annular liquid film, Equation (11) and (12) are combined by eliminating  $\frac{dP}{dz}$  as:

$$-\frac{\tau_F S_F}{A_F} + \tau_I S_I \left( \frac{1}{A_C} + \frac{1}{A_F} \right) - (\rho_L - \rho_G) g \sin \theta = 0 \quad (14)$$

where  $\tau_F$  and  $\tau_I$  are estimated by:

$$\tau_F = f_F \frac{\rho_F V_F^2}{2} \quad (15)$$

$$\tau_I = f_I \frac{\rho_C (V_G - V_F) |V_G - V_F|}{2} \quad (16)$$

where  $f_F$  is the wall fraction factor of the liquid and  $f_I$  is the interfacial fraction factor.  $f_F$  is estimated as follows [36]:

For laminar flow ( $Re < 2300$ ),

$$f_F = \frac{64}{Re_F} \quad (17)$$

For turbulent flow ( $Re \geq 2300$ ),

$$\frac{1}{\sqrt{f}} = -2 \log \left( \frac{k_s}{3.70d} + \frac{2.51}{Re_F \sqrt{f}} \right) \quad (18)$$

where  $k_s$  represents the surface roughness of the pipe.  $Re_F$  represents the Reynolds number at real liquid velocity in the annular region.

Several correlations were developed for predicting the interfacial fraction factor. Among them, Willis (1969) proposed a simple model to predict the interfacial friction factor using the film thickness.

$$f_I = 0.005 [1 + 300 \frac{\delta}{d}] \quad (19)$$

Or

$$f_I = 0.005 [1 + 75(1 - \alpha)] \quad (20)$$

where  $\alpha$  is the overall void fraction of the annular flow. Equation (20) works as long as the entrained liquid droplets could be ignorable ( $\alpha_C \rightarrow 1$ ).

By now, a hydrodynamic model of annular flows has been established. Compared with most of the existing models of two-phase annular flows which requires complicated numerical simulation, only a simple iteration in terms of the liquid film thickness is used in current model. The liquid film thickness is firstly assumed and substituted into the model to estimate the specific flow parameters, such as the pressure drop, overall void fraction, and actual flow velocities of liquid film and gas core, etc. Then, the assumed liquid film thickness will change and approach to the true value at each iteration step. When the calculated liquid film thickness approaches infinitely to the assumed value

$(\delta_{cal} - \delta_{ass}, i \leq 10^{-6})$  at the  $i^{\text{th}}$  step,  $\delta_{ass,i}$  is considered as the true value of the liquid film thickness. Then, the other flow parameters, such as  $V_G, V_D, V_F$ , and  $A_C$ , can be estimated using the calculated value of the liquid film thickness.

### 3. Heat transfer model

The schematic of the temperature field of the annular flow is shown in Fig. 2. The inlet temperature in annular film and gas core are  $T_{Fi}$  and  $T_{Ci}$ , and the outlet temperature are  $T_{Fo}$  and  $T_{Co}$ , respectively. The surrounding temperature is  $T_S$ .

As shown in Fig. 2, the heat transfer occurs at the pipe wall between the annular liquid film and the pipe wall and at the interface between the liquid film and the gas core. The contact area is  $A$  and  $A_C$ , respectively. Therefore, the energy balance equation of the liquid film in the control volume with the length of  $dL$  is formulated by:

$$(T_{Fo} - T_{Fi})C_{PF}V_FA_F\rho_F = -q_F S_F dL - q_I S_I dL \quad (21)$$

Or

$$\frac{\partial T_F}{\partial L} = -\frac{q_F S_F + q_I S_I}{C_{PF}V_FA_F\rho_F} \quad (22)$$

where  $q_F$  and  $q_I$  are the heat transfer fluxes between the annular liquid film and the pipe wall and between the annular liquid film and the gas core, respectively.

$$q_F = h_F(T_F - T_S) \quad (23)$$

$$q_I = h_I(T_F - T_C) \quad (24)$$

where  $h_F$  and  $h_I$  are the local heat transfer coefficients between the annular liquid film and the pipe wall and between the annular liquid film and the gas core, respectively.

The energy conservation equation of the gas core is formulated by:

$$(T_{Co} - T_{Ci})C_{PC}V_GA_C\rho_C = q_I S_I dL \quad (25)$$

Or

$$\frac{\partial T_C}{\partial L} = \frac{q_I S_I}{C_{PC}V_GA_C\rho_C} \quad (26)$$

Considering the equal temperature gradients of the annular liquid film and gas core in the control volume, combining Equations (22) and (26) by eliminating  $\frac{\partial T}{\partial L}$  yields:

$$\frac{C_{PC}V_GA_C\rho_C}{C_{PF}V_FA_F\rho_F}(q_F S_F + q_I S_I) = -q_I S_I \quad (27)$$

or

$$K(q_F S_F + q_I S_I) = -q_I S_I \quad (28)$$

where

$$K = \frac{C_{PG}V_GA_G\rho_G}{C_{PF}V_FA_F\rho_F} \quad (29)$$

Replacing  $q_F$  and  $q_I$  by Equations (23) and (24) in Equation (27) yields:

$$K[h_F(T_F - T_S)S_F + h_I(T_F - T_C)S_I] = h_I(T_F - T_C)S_I \quad (30)$$

The overall heat transfer flux is given as:

$$q_{2\Phi} = h_{2\Phi}(T_m - T_S)\pi d \quad (31)$$

Or

$$h_{2\Phi} = \frac{q_{2\Phi}}{(T_m - T_S)\pi d} \quad (32)$$

where  $T_m$  is the mass flow-based bulk temperature of the gas–liquid mixture.

Therefore, the next is to identify the local heat transfer coefficients at the pipe wall and gas–liquid interface. Gnielinski [20] proposed a correlation for predicting the heat transfer coefficients of turbulent flows ( $Re \geq 1 \times 10^4$ ) in concentric annular ducts. For annular two-phase flow, the liquid film flows in the annular region and thus Gnielinski correlation (2009) is just used to calculate the heat transfer coefficient of the annular liquid film. The expression of Gnielinski correlation is given by:

$$Nu = \frac{(f_{ann}/8)RePr}{k_1 + 12.7\sqrt{f_{ann}/8}(Pr^{2/3} - 1)}[1 + (\frac{d_H}{L})^{2/3}]F_{ann}k \quad (33)$$

where  $k_1$  and  $k$  are the parameters.

$$k_1 = 1.07 + \frac{900}{Re} - \frac{0.63}{1 + 10Pr} \quad (34)$$

$$K = \left(\frac{Pr_B}{Pr_W}\right)^{0.11} \quad (35)$$

The friction factor of the annulus flow,  $f_{ann}$ , is given as:

$$f_{ann} = (1.8\log_{10}Re^* - 1.5)^{-2} \quad (36)$$

$$Re^* = Re \frac{\left[1 + \left(\frac{d_i}{d_o}\right)^2\right]\ln\frac{d_i}{d_o} + \left[1 - \left(\frac{d_i}{d_o}\right)^2\right]}{\left[1 - \left(\frac{d_i}{d_o}\right)^2\right]\ln\frac{d_i}{d_o}} \quad (37)$$

where  $d_i$  and  $d_o$  are the diameters of the inner and outer tubes.

$F_{ann}$  is the factor to take into account the dependence on  $\frac{d_i}{d_o}$ .  $F_{ann}$  is estimated as follows. [20]:

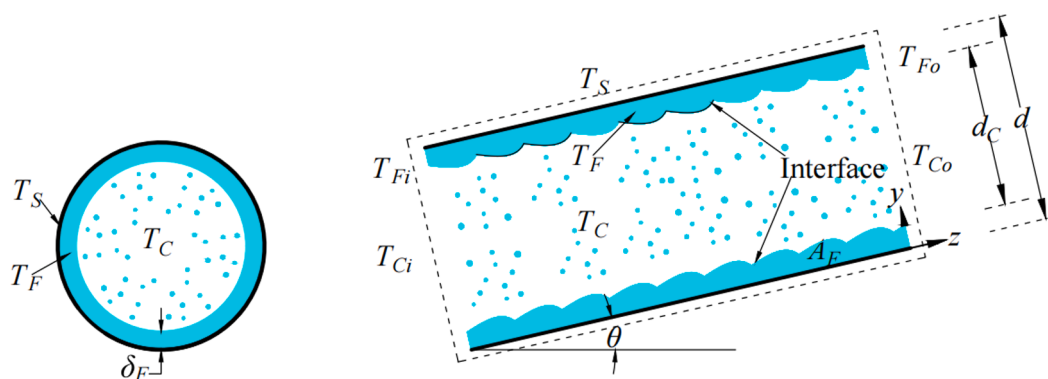


Fig. 2. Schematic of the temperature field in the control volume of annular flow.

$$F_{ann} = 0.9 - 0.15 \left( \frac{d_i}{d_o} \right)^{0.6} \quad (38)$$

For the laminar liquid film flow in concentric annular ducts, the heat transfer coefficients only depend on  $\frac{d_i}{d_o}$ . Table 1 presents the variation of Nusselt number on  $\frac{d_i}{d_o}$  for laminar falling film flows in concentric annular ducts [39]. Therefore, the heat transfer coefficients of laminar annular liquid film are determined using the interpolation method in terms of  $\frac{d_i}{d_o}$ . What's more, the interpolation method is also applied in identifying the heat transfer coefficients of transitional liquid film flow ( $2.3 \times 10^3 < Re_F < 1.0 \times 10^4$ ) in terms of  $Re_F$ .

As for the heat transfer coefficient at the interface, Zhang et al., [52] indicated that the interfacial heat transfer coefficients were equal to the heat transfer coefficients of the gas core.

$$h_I = h_C = \frac{Nu_C \lambda_C}{d_C} \quad (39)$$

where  $h_I$  is the heat transfer coefficient at the interface and  $h_C$  is the heat transfer coefficient of the gas core.  $Nu_C, \lambda_C$ , and  $d_C$  are the Nusselt number, thermal conductivity, and equivalent diameter of the gas core, respectively. Recently, Meyer et al. [30] developed a well-validated heat transfer correlation of laminar, transitional, quasi-turbulent, and turbulent flows in circular tubes based on a large amount of experimental data. Thus, Meyer et al. correlation (2019) is adopted to predict the heat transfer coefficient of the gas core. The expression of Meyer et al. correlation (2019) is given as follows.

For laminar flow.

$$Nu_C = 4.36 + Nu_{C1} + Nu_{C2} \quad (40)$$

where

$$Nu_{C1} = \frac{1}{L} \left[ -0.84 Pr_C^{-0.2} Lt_{MCD} + 0.72 (Re_C d_C)^{0.54} Pr_C^{0.34} Lt_{MCD}^{0.46} \right] \quad (41)$$

$$Nu_{C2} = \frac{1}{L} (0.207 Gr_C^{0.305} - 1.19) Pr_C^{0.42} (Re_C d_C)^{-0.08} (L - Lt_{MCD}) \quad (42)$$

where  $Lt_{MCD}$  is the mixed convection thermal entrance length and  $L$  is the pipe length.

$$Lt_{MCD} = \begin{cases} \frac{2.4 Re_C Pr_C^{0.6} d_C}{Gr_C^{0.57}} & \text{for } L > Lt_{MCD} \\ L & \text{for } L < Lt_{MCD} \end{cases} \quad (43)$$

For quasi-turbulent and turbulent flow

$$Nu_C = 0.018 Re_C^{-0.25} (Re_C - 500)^{1.07} Pr_C^{0.42} \left( \frac{Pr_C}{Pr_{C,w}} \right)^{0.11} \quad (44)$$

where  $Re_C, Pr_C$ , and  $Gr_C$  are the Reynolds number, Prandtl number, and Grashof number of the gas core, respectively.

To clearly demonstrate the heat transfer difference between two- and single-phase flows, a heat transfer multiplier,  $\Phi_h^2$ , defined as the ratio of two-phase heat transfer coefficient to single-phase heat transfer coefficient at the same liquid flow rates, is introduced.

$$\Phi_h^2 = \frac{h_{2\Phi}}{h_{1\Phi}} \quad (45)$$

At this point, a new model of flow and heat transfer for non-boiling two-phase annular flow is mathematically formulated. The influence of orientations and flow parameters, such as the pipe inclination angles, void fraction, superficial liquid and gas velocities, and pressure drop, on the heat transfer coefficients will be well examined in the next section.

## 4. Results and discussion

### 4.1. Model validation

To evaluate the predictive performance of the new model, the comparison between the experimental and calculated void fractions, liquid film thicknesses, and two-phase heat transfer coefficients is conducted in this section. Two statistical indices, namely, mean relative deviation,  $m_{rel}$ , and mean absolute relative deviation,  $m_{rel, ab}$ , are introduced to evaluate the predictive performance of the new model quantitatively. The definitions of these statistical indices are given as follows.

$$m_{rel} = \frac{1}{N} \sum_{i=1}^N \frac{|j_{cal} - j_{exp}|}{j_{exp}} \times 100\% \quad (46)$$

$$m_{rel, ab} = \frac{1}{N} \sum_{i=1}^N \frac{|j_{cal} - j_{exp}|}{j_{exp}} \times 100\% \quad (47)$$

where  $N$  is the number of the samples and  $j$  is the parameters, such as void fraction, liquid film thickness, and two-phase heat transfer coefficient.

The void fraction is one of the key parameters in annular flows. The accurate calculation of void fraction is very important to the analysis of flow mechanism. Fig. 3 presents the comparison between the simulated and experimental void fractions of annular flows. The experimental data were taken from Spedding and Nguyen [41], Mukherjee [32], Bhagwat and Chajer [3], Luo et al. [29], and Bhagwat and Chajer (2017). The pipe inclination angles ranges from  $-90^\circ$  to  $+90^\circ$ . The pipe diameter ranges from 0.0125 m to 0.0600 m. Both laminar and turbulent flows are involved. Fig. 3 indicates that all the void fractions are predicted within  $\pm 10\%$  errors without any systematic bias. The mean relative deviation is  $-1.50\%$  and mean absolute relative deviation is  $3.33\%$ .

The liquid flows in the annular-shaped channel as thin liquid film, forced by the gas core. Thus, the liquid film thickness is critical to the flow and heat transfer process. Fig. 4 presents the comparison of the experimental and simulated mean thickness of the liquid film. The experimental data were taken from Shedd and Newell [40], Wang et al. [49], and Uche [45]. Both laminar and turbulent flows are involved. Fig. 4 indicates that most of the mean thickness of the liquid film are predicted within  $\pm 20\%$  errors without any systematic bias. The mean relative deviation is  $-3.35\%$  and the mean absolute relative deviation is  $8.39\%$ .

Apart from the flow parameters, the accurate prediction of the heat transfer parameters is also very important. Fig. 5 presents the comparison of the experimental and simulated heat transfer coefficients of annular flows. The experimental data were collected from Rezkallah and Sims [37], Ghajar and Tang [18], Bhagwat and Ghajar [2], Nada [34], and Bhagwat and Ghajar [4]. Both laminar and turbulent flows are involved. 85.2 % of the heat transfer coefficients are predicted within  $\pm 20\%$  errors without any systematic bias. The mean relative deviation is  $-5.92\%$  and the mean absolute relative deviation is  $10.3\%$ .

The small discrepancy between simulated and experimental parameters results from several reasons, such as the adoption of empirical correlations for predicting entrainment rates and heat transfer coefficients, and the measurement uncertainties of the experimental data. However, most of the parameters are accurately predicted around the

**Table 1**  
Summary of the  $Nu$  number of laminar falling film in concentric annular ducts [39].

$d_i/d_o$	$Nu_i$ (Heat insulation of external surface)	$Nu_o$ (Heat insulation of internal surface)
0	/	3.66
0.05	17.46	4.06
0.10	11.56	4.11
0.25	7.37	4.23
0.50	5.74	4.53
1.00	4.86	4.86

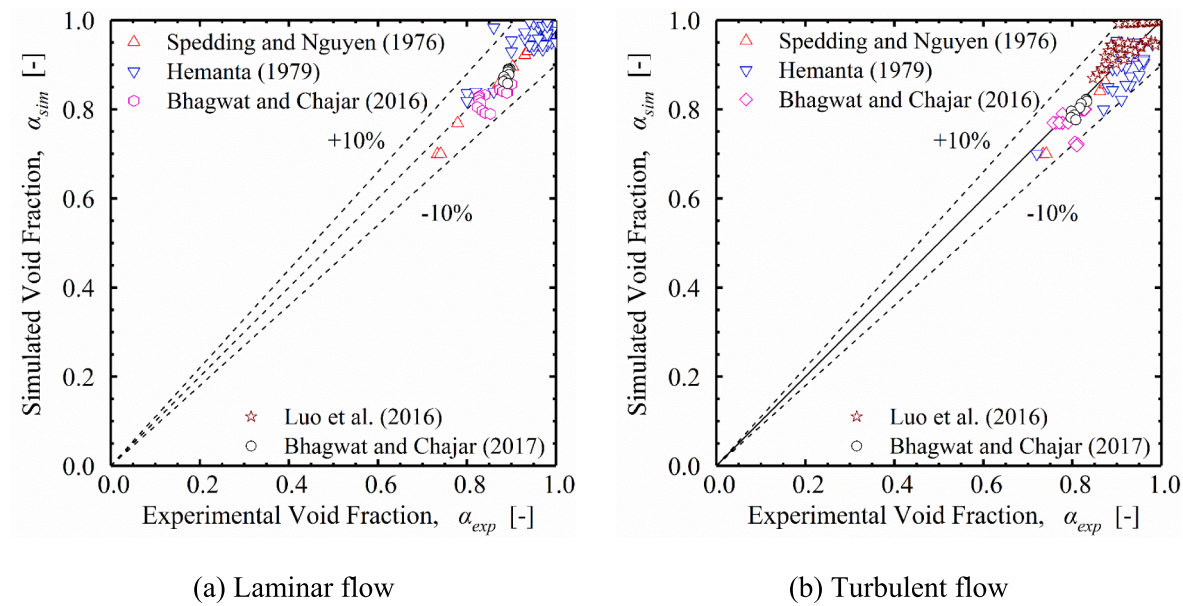


Fig. 3. Comparison of the simulated and experimental void fractions.

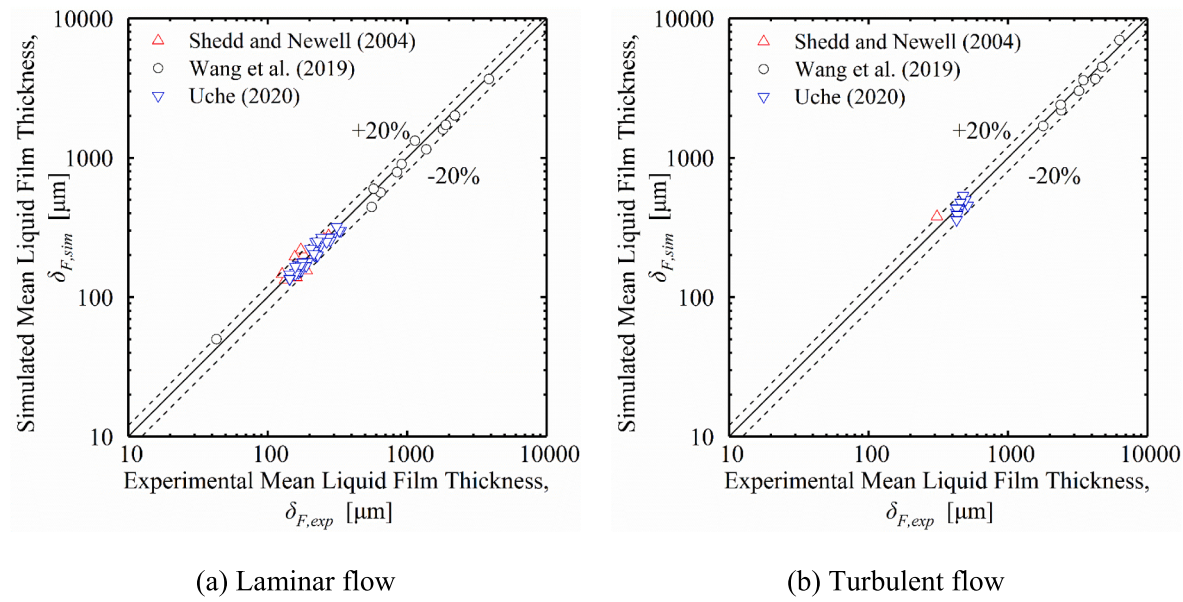


Fig. 4. Comparison of the simulated and experimental thickness of the liquid film.

experimental data without any systematic bias. In conclusion, the newly-developed model of flow and heat transfer for two-phase annular flow is well validated. The pipe orientations ranges from  $-90^\circ$  to  $+90^\circ$ . What's more, since no mass transfer between the liquid film and gas is considered, the new model is only suitable in predicting the flow and heat transfer performance of non-boiling two-phase flows.

#### 4.2. Effects of orientations and flow parameters on heat transfer coefficient

1200 flow conditions are simulated to analyze the effect of the local and overall orientations and flow parameters on the heat transfer process using the newly-developed model. The pipe diameter is selected as 0.0125 m. As stated by Bhagwat and Ghajar [4], two-phase annular flow occurs at high flow rates of gas and low-to-moderate flow rates of liquid. Fig. 6 shows part of the selected flow conditions ( $\theta = 0^\circ$ ) located in

Bhagwat and Ghajar [4] flow regime map. The selected superficial liquid velocity ranges from 0.03 m/s to 2.2 m/s and the superficial liquid Reynolds number ranges from  $4.70 \times 10^2$  to  $3.45 \times 10^4$ . Both laminar and turbulent liquid flows are involved. The selected superficial gas velocity ranges from 17 m/s to 50 m/s and the superficial gas Reynolds number ranges from  $1.47 \times 10^4$  to  $4.33 \times 10^4$ . To investigate the effect of pipe inclination angles on the heat transfer coefficients,  $\theta = 0^\circ, 5^\circ, 10^\circ, 20^\circ, 30^\circ, 45^\circ, 60^\circ, 70^\circ, 80^\circ$ , and  $90^\circ$  are simulated. Table 2 summarizes part of the simulated flow conditions ( $\theta = 90^\circ$ ).

##### 4.2.1. Superficial liquid Reynolds number

Fig. 7 presents the variation of the heat transfer coefficients,  $h_{2\Phi}$ , and two-phase heat transfer multiplier,  $\Phi_h$ , with the superficial liquid Reynolds number in horizontal pipes. The superficial liquid Reynolds number ranged from  $4.70 \times 10^2$  to  $3.45 \times 10^4$ . Fig. 7 indicates that the influencing mechanism of the superficial liquid Reynolds number on the

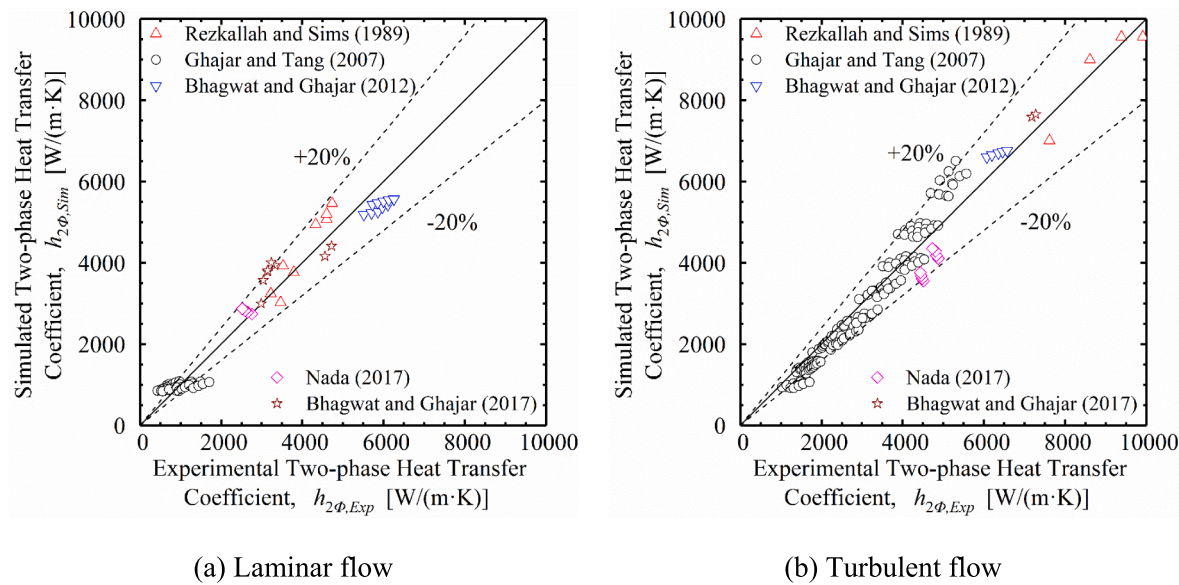


Fig. 5. Comparison of the simulated and experimental heat transfer coefficients.

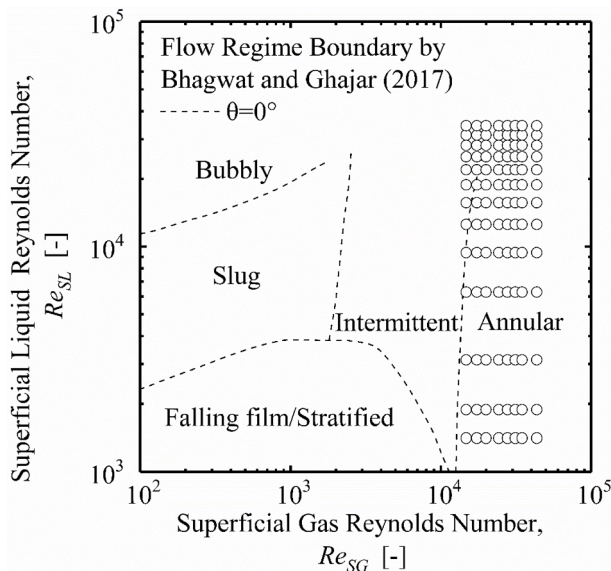


Fig. 6. Flow conditions in the flow regime map proposed by Bhagwat and Ghajar [4].

heat transfer process is quite complicated. To clearly express its influencing mechanism, the entire region is divided into three sub-regions.

In Region I, the two-phase heat transfer coefficient decreases with the increase of the superficial liquid velocity. The reason is the liquid film is laminar due to the low liquid flow rate in Region I and the heat transfer performance of the liquid film in the pipes with uniform cross section depends little on the  $Re_F$  [42] and only depends on  $d_i/d_o$  at laminar liquid film. As  $Re_{SL}$  increases, the liquid film thickness increases and the heat transfer performance is deteriorated, which is consistent with the expectation of higher heat transfer across a thin film. What's more, as shown in Fig. 7(b), the two-phase heat transfer multiplier is highest in the entire region. It means the enhancing effect of gas on the heat transfer process is most effective in Region I. The reason is when  $Re_{SL} < 2300$ , the flow is laminar flow and the injection of gas could effectively enhance the flow turbulence of the liquid film, rapidly reduce the resistance to heat transfer, and increase the heat transfer coefficient accordingly. Region I is considered as the turbulent-laminar two-phase

annular flow.

In Region II, the two-phase heat transfer multipliers decrease, while the two-phase heat transfer coefficients increase rapidly with the superficial liquid Reynolds number. The reason is as  $Re_{SL}$  increases, the intrinsic flow turbulence of liquid flow increases and the heat transfer process is intensified but the enhancing effect of gas on the heat transfer process is reduced compared with the two-phase flow in Region I. Region II is considered as the turbulent-transitional two-phase annular flow.

In Region III, the two-phase heat transfer multiplier continues decreasing, indicating that the enhancing effect of gas on the heat transfer process became less prominent. The reason is in Region III, the liquid flow is fully turbulent flow and the role of gas in improving the flow turbulence is reduced. However, all the two-phase heat transfer multipliers are higher than 1.0, indicating that the gas is still effective in enhancing the heat transfer process in Region III. Region III is considered as the turbulent-turbulent two-phase annular flow.

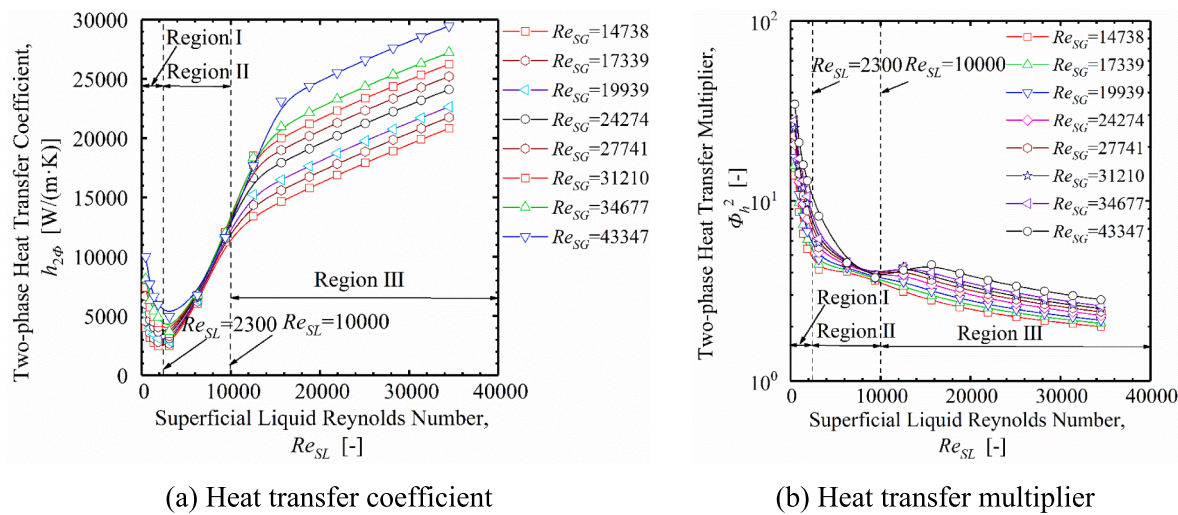
Fig. 8 presents the effect of the superficial liquid Reynolds number on the heat transfer of two-phase flows with different pipe inclination angles. The pipe inclination angle ranges from  $0^\circ$  to  $90^\circ$  and  $Re_{SG} = 14738$  is fixed. Although the heat transfer are similar in different pipe inclination angles, the heat transfer coefficient decreases slightly as the pipe inclination angles increase from  $0^\circ$  to  $90^\circ$ . The reason is due to the gravity effect, the velocity of the liquid film decreases with the increase of the pipe inclination angles, and the flow turbulence and heat transfer coefficient decrease as well.

#### 4.2.2. Superficial gas Reynolds number

Fig. 9 shows the effect of superficial gas Reynolds number on the heat transfer of two-phase annular flows. The superficial gas Reynolds number ranges from  $1.47 \times 10^4$  to  $4.33 \times 10^4$ . The influence of the superficial gas Reynolds number on the heat transfer varies in different regions. When  $Re_{SL} \leq 10000$  (laminar and transitional flows), the flow is not fully developed and the introduction of gas could significantly improve the flow turbulence. Thus, the two-phase heat transfer multipliers are as high as 6.59 and 3.64 at  $Re_{SL} = 470$  and  $Re_{SL} = 9408$ , respectively, with the first introduction of gas ( $Re_{SG} = 14738$ ), as shown in Fig. 9(b). The reason is when  $Re_{SL}$  is low, with a certain value of the liquid, more momentum is transferred from the gas to the liquid, and the enhancing effect is more pronounced at a low flow rate of the liquid. However, due to the low  $Re_{SL}$ , the first introduction of gas ( $Re_{SG} = 14738$ ) could improve the flow turbulence significantly and further

**Table 2**Summary of the simulated flow conditions at  $\theta = 90^\circ$ .

$V_{SL}$ [m/s]	$V_{SG}$ [m/s]	$h_{2\phi}$ [W/(m <sup>2</sup> ·K)]	$V_{SL}$ [m/s]	$V_{SG}$ [m/s]	$h_{2\phi}$ [W/(m <sup>2</sup> ·K)]	$V_{SL}$ [m/s]	$V_{SG}$ [m/s]	$h_{2\phi}$ [W/(m <sup>2</sup> ·K)]
0.03	17	1706.6	0.03	20	1898.0	0.03	23	2059.5
0.06	17	1839.9	0.06	20	2037.3	0.06	23	2205.1
0.09	17	1925.2	0.09	20	2125.9	0.09	23	2297.3
0.12	17	1988.9	0.12	20	2191.7	0.12	23	2365.6
0.20	17	2492.8	0.2	20	2669.0	0.2	23	2801.9
0.40	17	5796.8	0.4	20	6153.6	0.4	23	6428.0
0.60	17	10353.3	0.6	20	10883.7	0.6	23	11295.2
0.80	17	12579.2	0.8	20	13626.9	0.8	23	14608.2
1.	17	13857.1	1	20	14904.8	1	23	15891.0
1.2	17	15046.4	1.2	20	16090.3	1.2	23	17076.9
1.4	17	16170.6	1.4	20	17207.9	1.4	23	18191.9
1.6	17	17244.6	1.6	20	18273.2	1.6	23	19252.1
1.8	17	18278.6	1.8	20	19296.6	1.8	23	20268.6
2.0	17	19279.6	2	20	20285.6	2	23	21249.2
2.2	17	20253.1	2.2	20	21245.7	2.2	23	22199.6
0.03	28	2289.2	0.03	32	2449.8	0.03	36	2596.3
0.06	28	2444.1	0.06	32	2611.1	0.06	36	2763.1
0.09	28	2542.0	0.09	32	2713.0	0.09	36	2868.5
0.12	28	2614.5	0.12	32	2788.5	0.12	36	2946.7
0.2	28	2953.7	0.2	32	3029.0	0.2	36	3074.0
0.4	28	6741.2	0.4	32	6890.5	0.4	36	6970.0
0.6	28	11764.9	0.6	32	11984.5	0.6	36	12093.9
0.8	28	16116.8	0.8	32	17227.4	0.8	36	18100.2
1	28	17414.0	1	32	18539.1	1	36	19593.2
1.2	28	18606.5	1.2	32	19739.6	1.2	36	20803.0
1.4	28	19722.4	1.4	32	20859.1	1.4	36	21927.6
1.6	28	20779.5	1.6	32	21916.6	1.6	36	22986.8
1.8	28	21789.7	1.8	32	22924.6	1.8	36	23994.2
2	28	22761.3	2	32	23892.0	2	36	24959.0
2.2	28	23700.5	2.2	32	24825.4	2.2	36	25888.2
0.03	40	2731.9	1.4	40	22935.4	0.4	50	6869.2
0.06	40	2903.4	1.6	40	2397.3	0.6	50	11867.6
0.09	40	3012.0	1.8	40	25005.0	0.8	50	17682.3
0.12	40	3092.5	2	40	25968.3	1	50	22841.0
0.2	40	3095.4	2.2	40	26894.4	1.2	50	24084.6
0.4	40	6993.1	0.03	50	3036.5	1.4	50	25229.7
0.6	40	12113.3	0.06	50	3217.2	1.6	50	26299.6
0.8	40	18096.4	0.09	50	3332.1	1.8	50	27310.1
1	40	20585.6	0.12	50	3417.5	2	50	28271.9
1.2	40	21805.1	0.2	50	3576.5	2.2	50	29193.1

**Fig. 7.** Effect of superficial liquid Reynolds number on heat transfer of two-phase annular flow in horizontal pipes.

increase in gas flow rate could not result in pronounced increase in the absolute two-phase heat transfer coefficient, as shown in Fig. 9(a). When  $Re_{SL} > 10000$ , the flow is fully developed and higher gas flow rate is required to improve its flow turbulence. Thus, due to the high  $Re_{SL}$ , further increase in the gas flow rate could result in pronounced increase

in the absolute two-phase heat transfer coefficient, as shown in Fig. 9(a).

#### 4.2.3. Reynolds number and thickness of liquid film

In two-phase annular flow, the liquid is assumed to flow in the annular-shaped channel as liquid film. Thus, the local flow parameters

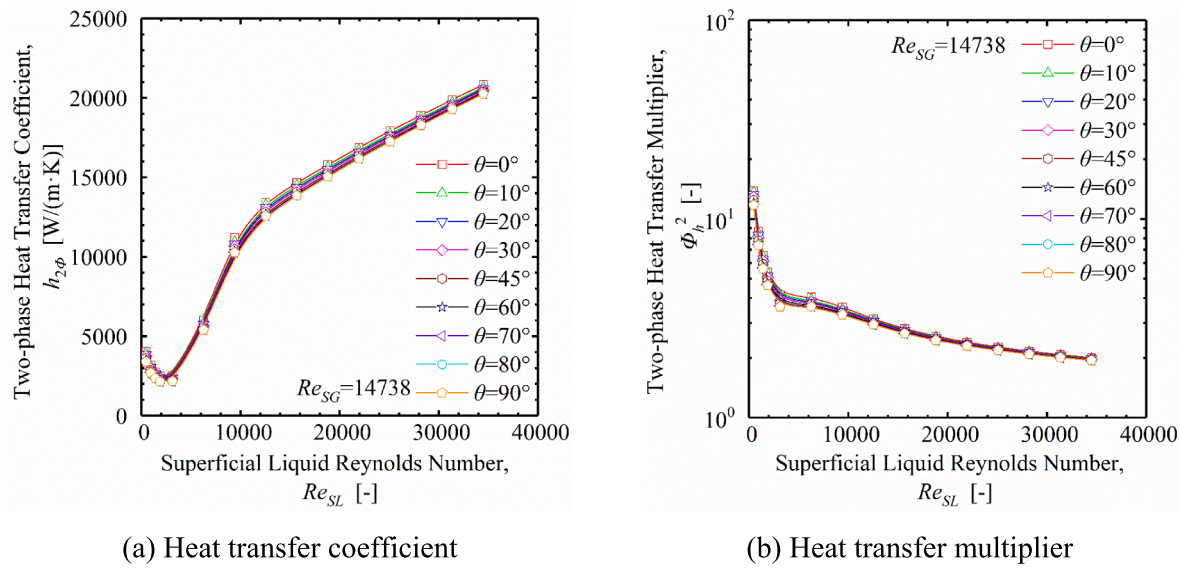


**Fig. 8.** Effect of superficial liquid Reynolds number on heat transfer of two-phase annular flow in different pipe inclination angles.

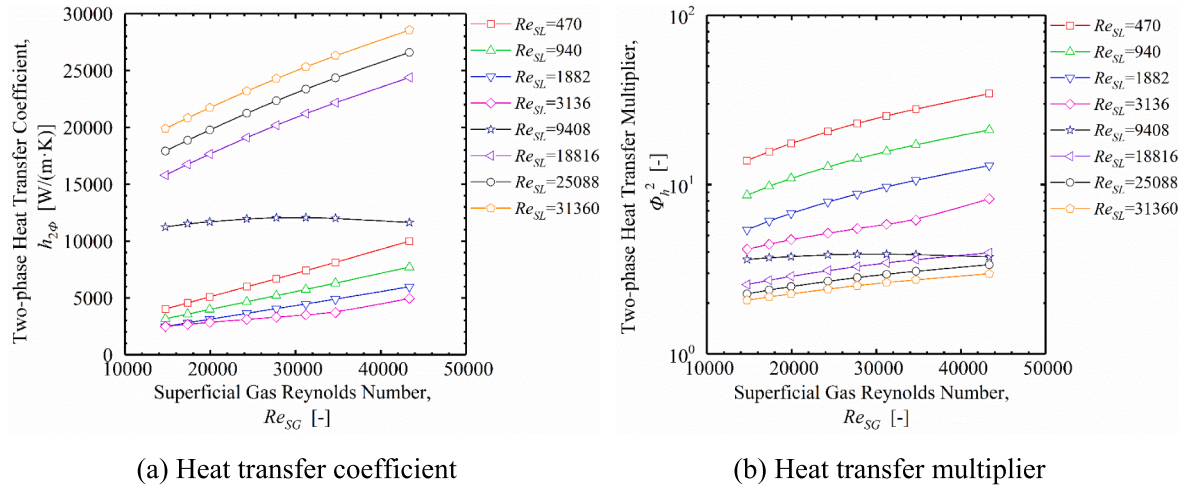


**Fig. 9.** Effect of the superficial gas Reynolds number on the two-phase heat transfer coefficients.

of the liquid film, such as the Reynolds number and thickness, are important to the heat transfer process. Due to the interrelated relationship between the film thickness, two-phase heat transfer coefficient, and film flow rate, 3-D plots in terms of two-phase heat transfer coefficient/multiplier, film thickness, and Reynolds number of liquid film is adopted. Fig. 10 presents the dependence of two-phase heat transfer multiplier on the liquid film thickness and Reynolds number of the liquid film. The two-phase heat transfer multipliers first decrease rapidly then slightly with both the Reynolds number and liquid film thickness. This is because as  $Re_f$  increases, the intrinsic flow turbulence increases and the enhancing effect of gas becomes less prominent. What's more, as  $\delta_f$  increases, the gas flow only accelerates the interfacial liquid instead of the interior liquid close to the pipe wall, which also attenuate the enhancing effect.

#### 4.2.4. Void fraction and pressure drop

Fig. 11 shows the variation of the two-phase heat transfer multipliers with the void fractions. The liquid holdup,  $1-\alpha$ , is used in the figure. Apparently, the two-phase heat transfer multiplier depends heavily on the void fraction. As the void fraction decreases (liquid holdup increases), the two-phase heat transfer multiplier decreases rapidly.

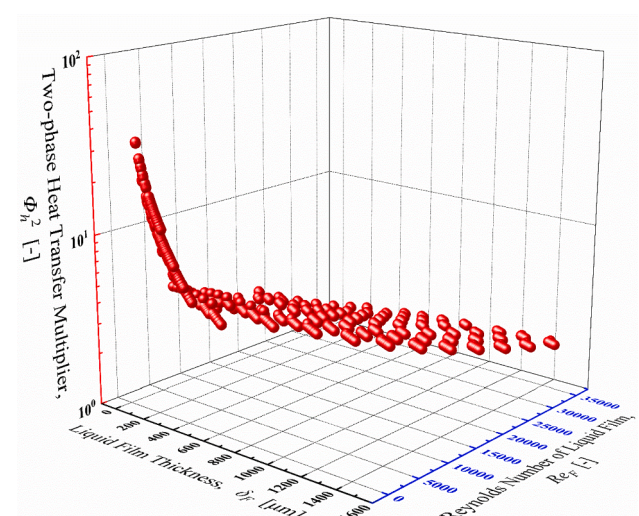


**Fig. 10.** Effect of the Reynolds number and thickness of liquid film on two-phase heat transfer multiplier.

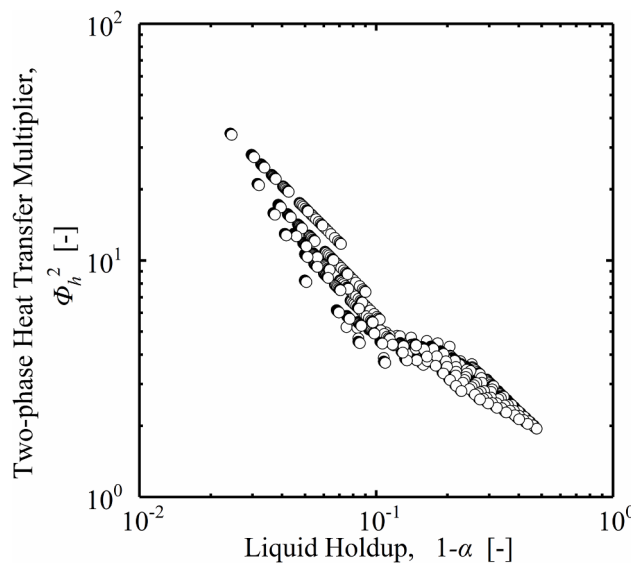


**Fig. 11.** Effect of the void fraction on two-phase heat transfer multiplier.

What's more,  $\Phi_h^2$  approaches 1.0, as  $\alpha$  approaches 0 infinitely. It is physically correct, since  $\alpha \rightarrow 0$  means the two-phase flow approaches single-phase flow and the two-phase heat transfer coefficient approaches single-phase heat transfer coefficient.

The pressure drop multiplier,  $\Phi_f^2$ , defined as the ratio of the pressure drop of two-phase flow to that of single-phase flow, is used in the analysis. Fig. 12 shows that the two-phase heat transfer multipliers depend heavily on the pressure drop multipliers. The heat transfer multipliers increase rapidly with the pressure drop multipliers. What's more,  $\Phi_h^2$  approaches 1.0, as  $\Phi_f^2$  approaches 1.0 infinitely. It is physically correct, since  $\Phi_f^2 \rightarrow 1.0$  means the two-phase flow approaches single-phase flow and the two-phase heat transfer coefficient approaches single-phase heat transfer coefficient.

Chilton & Colburn analogy indicates that the heat transfer is analogous to the momentum transfer [53,50]. Recently, Dong and Hibiki [10,11] derived a formulation to express the relationship between the heat transfer multipliers, void fractions and pressure drop multipliers

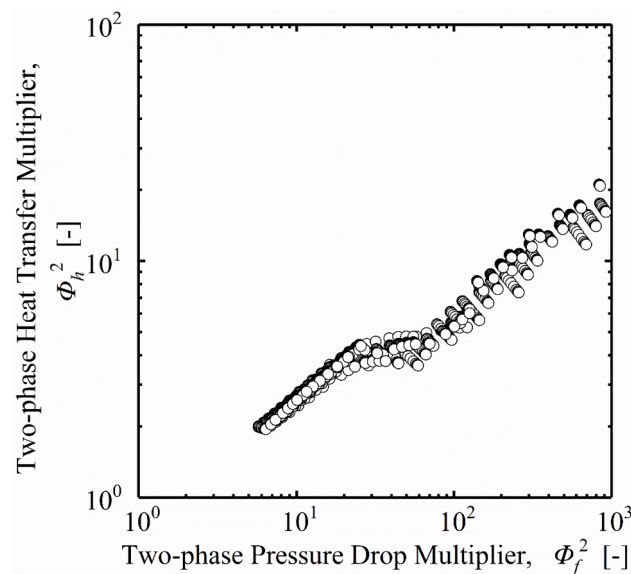


**Fig. 12.** Effect of the pressure drop multiplier on two-phase heat transfer multiplier.

using the Chilton-Colburn analogies. The formulation is expressed as:

$$\Phi_h^2 = (1 - \alpha)^m \left( \Phi_f^2 \right)^n \quad (48)$$

where  $m$  and  $n$  are the exponents. Here,  $m$  and  $n$  are determined using the simulated data. Thus, the relationship between the heat transfer multiplier and the pressure drop multiplier is quantitatively expressed as:

$$\Phi_h^2 = (1 - \alpha)^{-0.0652} \left( \Phi_f^2 \right)^{0.400} \quad (49)$$

**Fig. 13** evaluates the predictive performance of the new correlation. The calculated heat transfer multiplier refers to the value calculated by the new correlation, Equation (49), and the simulated heat transfer multiplier refers to the value calculated by the model, as expressed in Sections 2 and 3. As shown in Fig. 13, although a very simple formulation is used, most of the data fall within  $\pm 20\%$  errors without any systematic bias. What's more, Equation (47) also achieve the aptitude that when  $\Phi_f^2$  approaches 1.0 and  $\alpha$  approaches 0,  $\Phi_h^2$  could approach 1.0.

## 5. Conclusions

This paper developed a model of flow and heat transfer for turbulent-laminar/turbulent gas–liquid two-phase annular flows. The flow and heat transfer behaviors of two-phase annular flow are investigated. The effect of orientations and flow parameters, such as the superficial Reynolds numbers of the liquid and gas, Reynolds number and thickness of liquid film, void fraction, pressure drop, and inclination angles, on the heat transfer coefficients were investigated extensively. The achievements are as follows:

- (1) The physical process of flow and heat transfer for annular flow was mathematically formulated. A model of flow and heat transfer for turbulent-laminar/turbulent two-phase annular flows was developed. The new model achieves both simplicity and high accuracy.
- (2) The heat transfer enhancement by the injection of gas into liquid was investigated comprehensively. The two-phase heat transfer multiplier decreased with the superficial liquid Reynolds number, but increased with the superficial gas Reynolds number.
- (3) The relationships between the two-phase heat transfer multipliers and the void fractions and pressure drop multipliers were

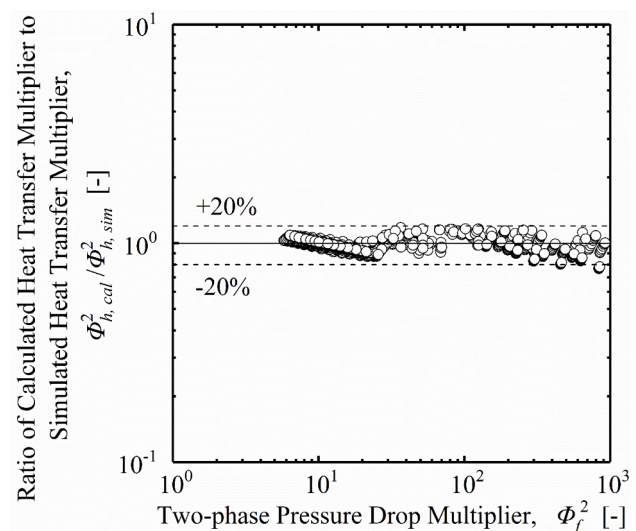


**Fig. 13.** Comparison between the simulated and calculated two-phase heat transfer multipliers.

identified quantitatively. A simple correlation of heat transfer multiplier was developed based on Chilton & Colburn analogy and a large amount of data, acting as a rough but quick prediction of the heat transfer multipliers of two-phase annular flows.

## Data availability

The data that support the findings of this study are available from the corresponding author upon reasonable request.

## Declaration of Competing Interest

The authors declare that they have no known competing financial interests or personal relationships that could have appeared to influence the work reported in this paper.

## Data availability

Data will be made available on request.

## Acknowledgments

The project is supported by the National Natural Science Foundation of China (NSFC), No. 51906071 and No. 51936005; the Natural Science Foundation of Guangdong Province, No. 2019A1515011536; Young Talent Support Project of Guangzhou Association for Science and Technology.

## References

- [1] A.M. Aliyu, Y.D. Baba, L. Lao, H. Yeung, K. Kim, Interfacial friction in upward annular gas-liquid two-phase flow in pipes, *Exp. Therm. Fluid Sci.* 84 (2017) 90–109.
- [2] S.M. Bhagwat, A.J. Ghajar, Similarities and differences in the flow patterns and void fraction in vertical upward and downward two phase flow, *Exp. Therm. Fluid Sci.* 39 (2012) 213–227.
- [3] S.M. Bhagwat, A.J. Ghajar, Experimental investigation of non-boiling gas liquid two phase flow in upward inclined pipes, *Exp. Therm. Fluid Sci.* 79 (2016) 301–318.
- [4] S.M. Bhagwat, A.J. Ghajar, Experimental investigation of non-boiling gas-liquid two phase flow in downward inclined pipes, *Exp. Therm. Fluid Sci.* 89 (2017) 219–237.
- [5] C. Chalons, M. Girardin, S. Kokh, An all-regime Lagrange-Projection like scheme for 2D homogeneous models for two-phase flows on unstructured meshes, *J. Comput. Phys.* 335 (2017) 885–904.
- [6] A. Cioncolini, J.R. Thome, Void fraction prediction in annular two-phase flow, *Int. J. Multiph. Flow* 43 (2012) 72–84.
- [7] A. Clausse, M.L. Bertodano, Natural modes of the two-fluid model of two-phase flow, *Phys. Fluids* 33 (2021), 033324.
- [8] Deendarlanto, A. Rahmandika, A. Widyatama, O. Dinaryanto, A. Widyaparaga, Indarto, Experimental study on the hydrodynamic behavior of gas-liquid air-water two-phase flow near the transition to slug flow in horizontal pipes, *Int. J. Heat Mass Tran.* 130 (2019) 187–203.
- [9] C. Dong, T. Hibiki, Correlation of heat transfer coefficient for two-component two-phase slug flow in a vertical pipe, *Int. J. Multiphase Flow* 108 (2018) 124–139.
- [10] C. Dong, T. Hibiki, Heat transfer correlation for two-component two-phase slug flow in horizontal pipes, *Appl. Therm. Eng.* 141 (2018) 866–876.
- [11] C. Dong, R. Qi, L. Zhang, Flow and heat transfer for a two-phase slug flow in horizontal pipes: A mechanistic model, *Phys. Fluids* 33 (2021), 034117.
- [12] C. Dong, R. Qi, L. Zhang, Mechanistic modeling of flow and heat transfer in turbulent-laminar/turbulent gas-liquid stratified flow, *Phys. Fluids* 33 (7) (2021) 073313.
- [13] C. Dong, R. Qi, L. Zhang, Mechanistic modelling of flow and heat transfer in vertical upward two-phase slug flows, *Phys. Fluids* 34 (2022), 013309.
- [14] C. Dong, S. Rassame, L. Zhang, T. Hibiki, Drift-flux correlation for upward two-phase flow in inclined pipes, *Chem. Eng. Sci.* 213 (2020), 115395.
- [15] W. Fan, C. Li, L. Li, X. Zhang, M. Du, X. Yin, Hydrodynamics of gas/shear-thinning liquid two-phase flow in a co-flow mini-channel: Flow pattern and bubble length, *Phys. Fluids* 32 (2020), 092004.
- [16] A.J. Ghajar, C.C. Tang, Heat transfer measurements, flow pattern maps and flow visualization for non-boiling two-phase flow in horizontal and slightly inclined pipes, *Heat Transf. Eng.* 28 (6) (2007) 525–540.
- [17] V. Gnielinski, Heat transfer coefficients for turbulent flow in concentric annular ducts, *Heat Transf. Eng.* 30 (6) (2009) 431–436.
- [18] H. He, L. Pan, Q. Ren, T. Ye, D. Zhang, Local liquid film behavior of annular two-phase flow on rod-bundle geometry-II. Modeling and verification, *Int. J. Heat Mass Tran.* 143 (2019), 118533.
- [19] H. He, L. Pan, Q. Ren, T. Ye, D. Zhang, Local liquid film behavior of annular two-phase flow on rod-bundle geometry-I. Experimental phenomenon and analysis, *Int. J. Heat Mass Tran.* 141 (2019) 58–70.
- [20] M. Ishii, T. Hibiki (Eds.), *Thermo-Fluid Dynamics of Two-Phase Flow*, Springer New York, New York, NY, 2010.
- [21] D. Ito, P. Papadopoulos, H.M. Prasser, Liquid film dynamics of two-phase annular flow in square and tight lattice subchannels, *Nucl. Eng. Des.* 300 (2016) 467–474.
- [22] P. Ju, Y. Liu, X. Yang, M. Ishii, Wave characteristics of vertical upward adiabatic annular flow in pipes, *Int. J. Heat Mass Tran.* 145 (2019), 118701.
- [23] N. Kattan, J.R. Thome, D. Favrat, Flow boiling in horizontal tubes. Part 1: Development of adiabatic two-phase flow pattern map, *J. Heat Transfer* 120 (1998) 140–147.
- [24] K. Keniar, S. Garimella, Modeling of annular and intermittent flow condensation in micro- and mini-channels with experimental validation, *Int. J. Heat Mass Tran.* 176 (2021), 121507.
- [25] P. Kumar, A.K. Das, S.K. Mitra, Physical understanding of gas-liquid annular flow and its transition to dispersed droplets, *Phys. Fluids* 28 (2016), 072101.
- [26] W. Luo, Y. Li, Q.H. Wang, J.L. Li, R.Q. Liao, Z.L. Liu, Experimental study of gas-liquid two-phase flow for high velocity in inclined medium size tube and verification of pressure calculation methods, *Int. J. Heat Technol.* 34 (3) (2016) 455–464.
- [27] J.P. Meyer, M. Everts, N. Coetze, K. Grote, M. Steyn, Heat transfer coefficients of laminar, transitional, quasi-turbulent and turbulent flow in circular tubes, *Int. Commun. Heat Mass Transf.* 105 (2019) 84–106.
- [28] T.A. Moreira, R.W. Morse, K.M. Dressler, G. Ribatski, A. Berson, Liquid-film thickness and disturbance-wave characterization in a vertical, upward, two-phase annular flow of saturated R245fa inside a rectangular channel, *Int. J. Multiph. Flow* 132 (2020) 103412.
- [29] H. Mukherjee, An experimental study of inclined two-phase flow, *The University of Tulsa, Tulsa, USA*, 1979.
- [30] S. Mukhopadhyay, G. Nimbalkar, Fundamental study on chaotic transition of two-phase flow regime and free surface instability in gas deaeration process, *Exp. Comput. Multiph. Flow* 3 (4) (2021) 258–288.
- [31] S.A. Nada, Experimental investigation and empirical correlations of heat transfer in different regimes of air-water two-phase flow in a horizontal tube, *J. Therm. Sci. Eng. Appl.* 9 (2017), 021004-1-7.
- [32] N. Panicker, A. Passalacqua, R.O. Fox, Computational study of buoyancy driven turbulence in statistically homogeneous bubbly flows, *Chem. Eng. Sci.* 216 (2020), 115546.
- [33] M.C. Potter, D.C. Wiggert, B.H. Ramadan, *Engineering Fluids Mechanics*, 4th ed., Cengage Learning, 2012.
- [34] K.S. Rezkallah, G.E. Sims, New data on two-phase, two-component heat transfer and hydrodynamics in a vertical tube, *J. Thermophys. 3* (2) (1989) 213–219.
- [35] A. Saxena, H.M. Prasser, A study of two-phase annular flow using unsteady numerical computations, *Int. J. Multiph. Flow* 126 (2020), 103037.
- [36] R.K. Shah, A.L. London, *Laminar flow forced convection in ducts*, Academic Press, 1978.
- [37] T. Shedd, T.A. Newell, Characteristics of the liquid film and pressure drop in horizontal, annular, two-phase flow through round, square and triangular tubes, *J. Fluid Eng.* 126 (2004) 807–817.
- [38] L. Spedding, V.T. Nguyen, Data on holdup, pressure loss and flow patterns for two-phase air water flow in an inclined pipe, *University of Auckland, Auckland New Zealand Report Eng.*, 1976, p. 122.
- [39] W.Q. Tao, *Heat Transfer Engineering*, Higher Education Press, 5th Edition., 2019.
- [40] J.R. Thome, Update on advances in flow pattern based two-phase heat transfer models, *Exp. Therm. Fluid Sci.* 29 (2005) 341–349.
- [41] J.R. Thome, *Encyclopedia of two-phase heat transfer and flow I*, World Scientific, 2016.
- [42] O. Uche, Evaluation of liquid film thickness in gas-liquid annular flow in horizontal pipes using three methods, *Int. J. Energy Environ. Sci.* 5 (4) (2020) 57–65.
- [43] K. Ueyama, A study of two-fluid model equations, *J. Fluid Mech.* 690 (2012) 474–498.
- [44] G.B. Wallis, *One dimensional two-phase flow*, McGraw-Hill, New York, 1969.
- [45] G. Wang, Z. Deng, M. Ishii, Wave structure and velocity in vertical upward annular two-phase flow, *Exp. Therm. Fluid Sci.* 120 (2021), 110205.
- [46] M. Wang, D.D. Zheng, Y. Xu, Z.Q. Cui, Liquid film thickness measurement for gas-liquid two phase flow using ultrasound. 2019 IEEE International Instrumentation and Measurement Technology Conference (I2MTC), 2019.
- [47] C. Wenzel, T. Gibis, M. Kloker, U. Rist, Reynolds analogy factor in self-similar compressible turbulent boundary layers with pressure gradients, *J. Fluid Mech.* 907 (2021) R4.
- [48] F. Xie, X. Zheng, M.S. Triantafyllou, Y. Constantinides, Y. Zheng, G.E. Karniadakis, Direct numerical simulations of two-phase flow in an inclined pipe, *J. Fluid Mech.* 825 (2017) 189–207.
- [49] H. Zhang, Q. Wang, C. Sarica, J.P. Brill, Unified model of heat transfer in gas-liquid pipe flow, *SPE Prod. Oper.* (2006) 114–122.

- [53] Y. Zhang, W. Bi, F. Hussain, Z. She, A generalized Reynolds analogy for compressible wall-bounded turbulent flows, *J. Fluid Mech.* 739 (2014) 392–420.
- [54] Z. Zhang, Z. Wang, H. Liu, Y. Gao, B. Sun, Experimental study on entrained droplets in vertical two-phase churn and annular flows, *Int. J. Heat Mass Tran.* 138 (2019) 1346–1358.
- [55] A.H. Zitouni, A. Arabi, Y. Salhi, Y. Zenati, E.K. Si-Ahmed, J. Legrand, Slug length and frequency upstream a sudden expansion in gas-liquid intermittent flow, *Exp. Comput. Multiph. Flow* 3 (2) (2021) 124–130.